Supplementary Material

Characterizing Open-Ended Evolution Through Undecidability Mechanisms in Random Boolean Networks

Amahury J. López-Díaz[1], Pedro Juan Rivera Torres[2], Gerardo Febres[1,3], and Carlos Gershenson[1]

[1] *School of Systems Science and Industrial Engineering, Binghamton University, 4400 Vestal Pkwy E, Binghamton, NY 13902, USA*

[2] *Department of Computer Science and Automation, University of Salamanca, 1 Patio de Escuelas, Salamanca, 37008, Spain*

[3] *Department of Processes and Systems, Universidad Simón Bolívar, C479+36J, Caracas, Miranda, Venezuela*

alpez@binghamton.edu

December 16, 2025

The present document includes experiments we have carried out for the paper "Characterizing Open-Ended Evolution Through Undecidability Mechanisms in Random Boolean Networks," where we explore the behavior of open-endedness using multiple mechanisms based on non-classical logics.

Abstract

Discrete dynamical models underpin systems biology, but we still lack substrate-agnostic diagnostics for when such models can sustain genuinely open-ended evolution (OEE): the continual production of novel phenotypes rather than eventual settling. We introduce a simple, model-independent metric, Ω, that quantifies OEE as the residence-time-weighted contribution of each attractor's cycle length across the sequence of attractors realized over time. Ω is zero for single-attractor dynamics and grows with the number and persistence of distinct cyclic phenotypes, separating enduring innovation from transient noise. Using Random Boolean Networks (RBNs) as a unifying testbed, we compare classical Boolean dynamics with biologically motivated non-classical mechanisms (probabilistic context switching, annealed rule mutation, paraconsistent logic, modal necessary/possible gating, and quantum-inspired superposition/entanglement) under homogeneous and heterogeneous update schemes. Our results support the view that undecidability-adjacent, state-dependent mechanisms—implemented as contextual switching, conditional necessity/possibility, controlled contradictions, or correlated branching—are enabling conditions for sustained novelty. At the end of our manuscript we outline a practical extension of Ω to continuous/hybrid state spaces, positioning Ω as a portable benchmark for OEE in discrete biological modeling and a guide for engineering evolvable synthetic circuits.

Shared experimental backbone (see Methods and Results in main text): unless stated otherwise, each point averages 1,000 independently sampled networks with $N = 100$ nodes, a random initial condition, mean connectivity $K \in [1.1, 4.5]$ in steps of 0.2, and horizon $T = 10^6$ time steps. The open-endedness metric is $\Omega = \frac{1}{T^2}\sum_{j=1}^{m} d_j k_j$, the residence-time-weighted sum of the cycle-lengths of each attractor A_j found within the window.

Horizon sensitivity (homogeneous and heterogeneous)

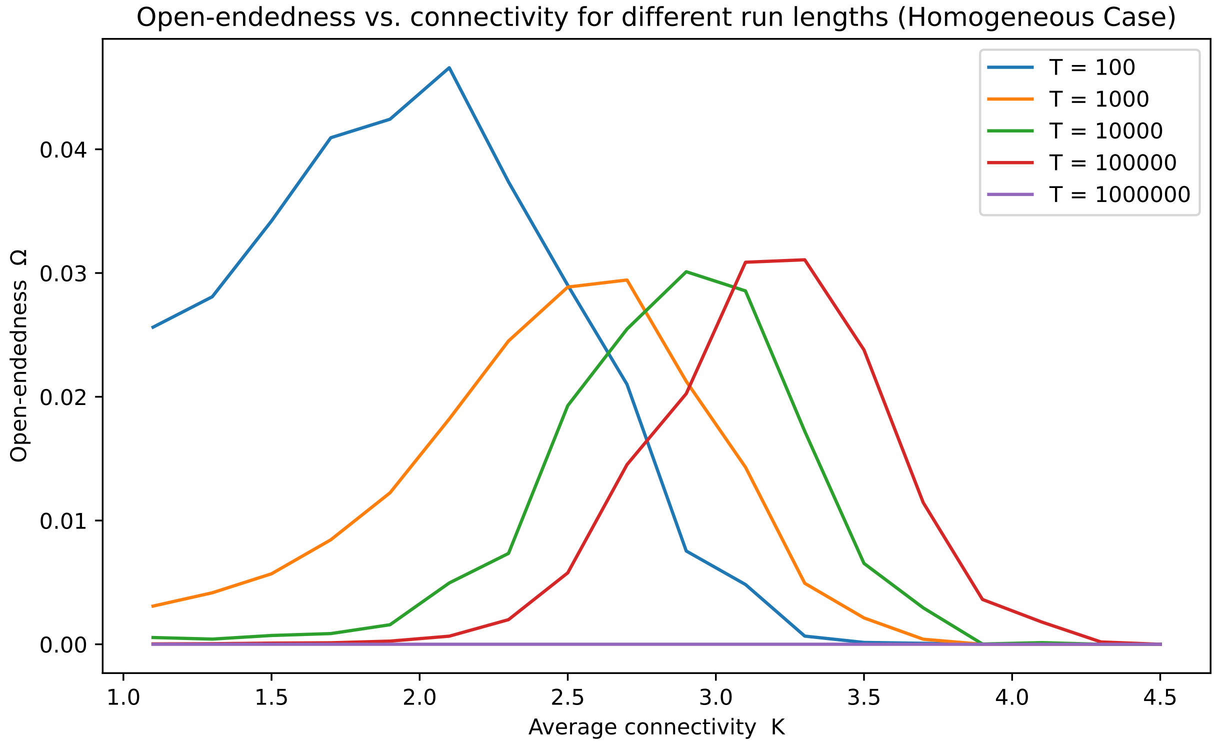

Figure 1: **Horizon (T) sensitivity of $\Omega(K)$ under homogeneous settings.** Each curve shows the mean Ω across 1,000 networks at fixed K for different simulation lengths T (legend as plotted in the notebook). Curves largely overlap beyond the smallest T, indicating that $T = 10^6$ suffices to stabilize $\Omega(K)$ in this regime. Axes: x–axis is average connectivity K; y–axis is open-endedness Ω (dimensionless, residence-time-weighted cycle-length normalized by T^2).

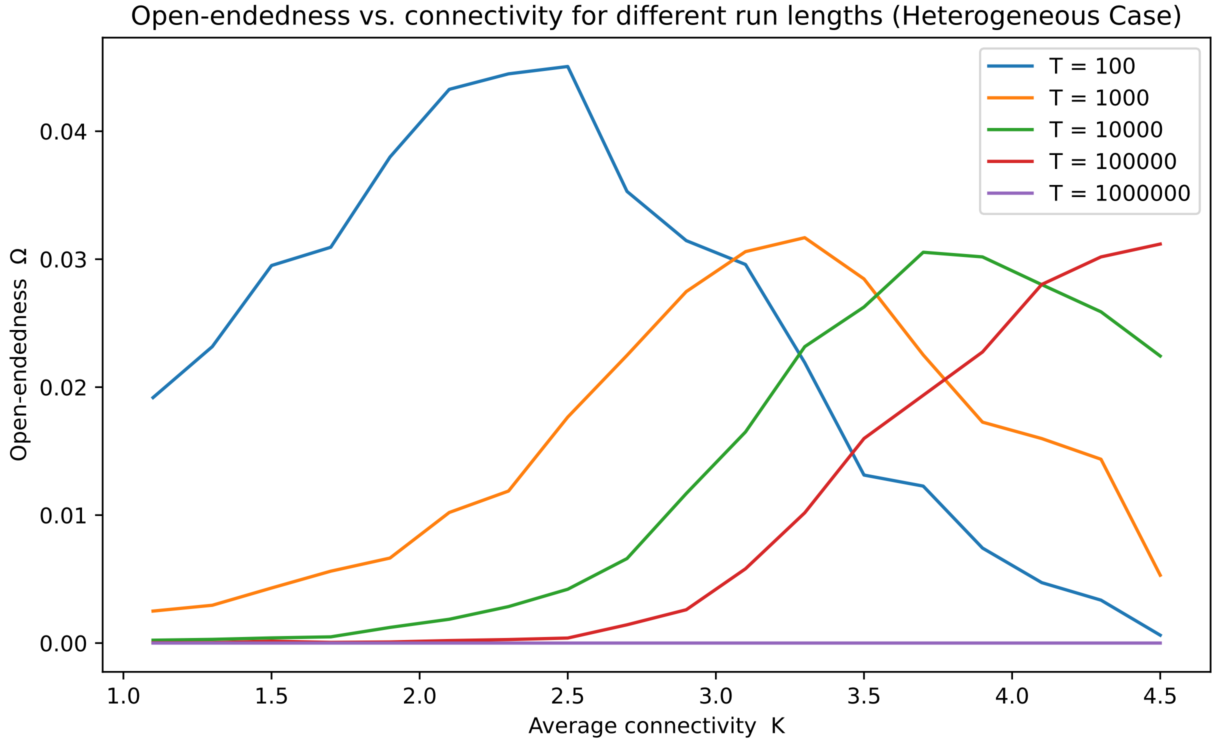

Figure 2: **Horizon (T) sensitivity of $\Omega(K)$ under heterogeneous settings.** Same protocol as Fig. 1 but with Exponential in-degree and asynchronous updates. Ω remains near zero across K at long T when dynamics collapse to fixed points, justifying the large-T choice used elsewhere.

Probabilistic Boolean Networks (PBN): context count and switching probability

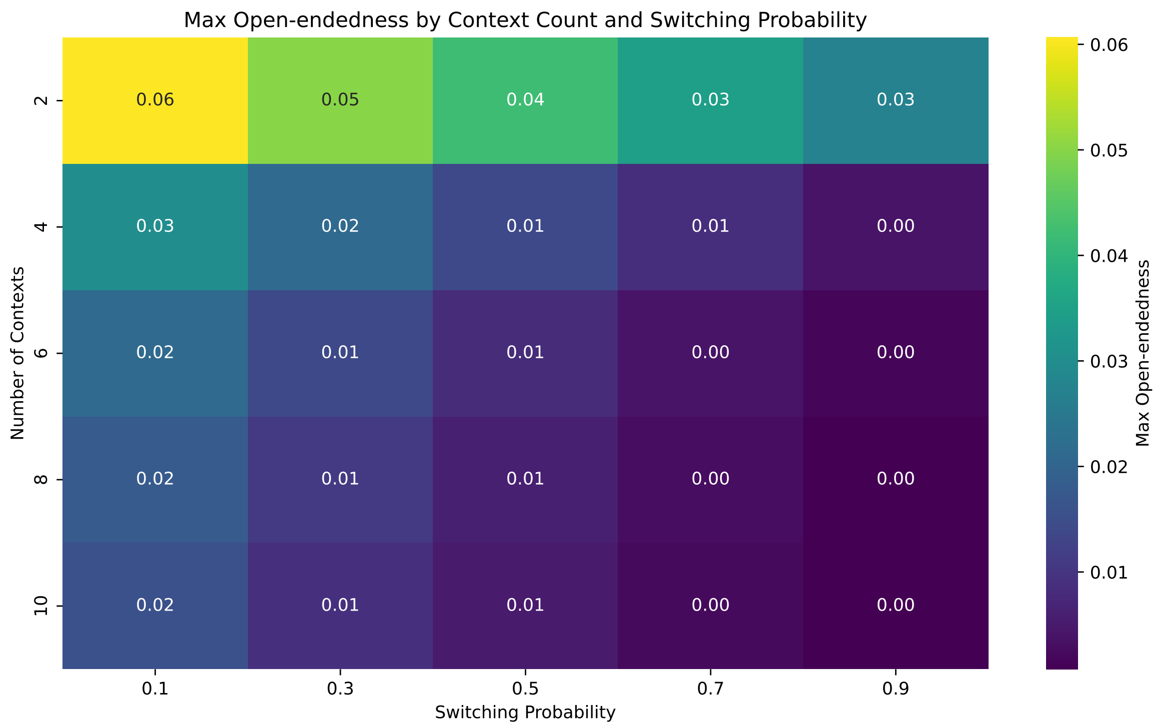

Figure 3: **Maximum observed Ω over K as a function of PBN switching probability σ (x-axis) and number of deterministic contexts (y-axis).** Higher counts allow more distinct attractor families but excessive switching suppresses dwell times; a sweet spot emerges at low σ with few contexts. Color scale: maximum mean Ω attained across the K grid for each $(\sigma, \text{contexts})$.

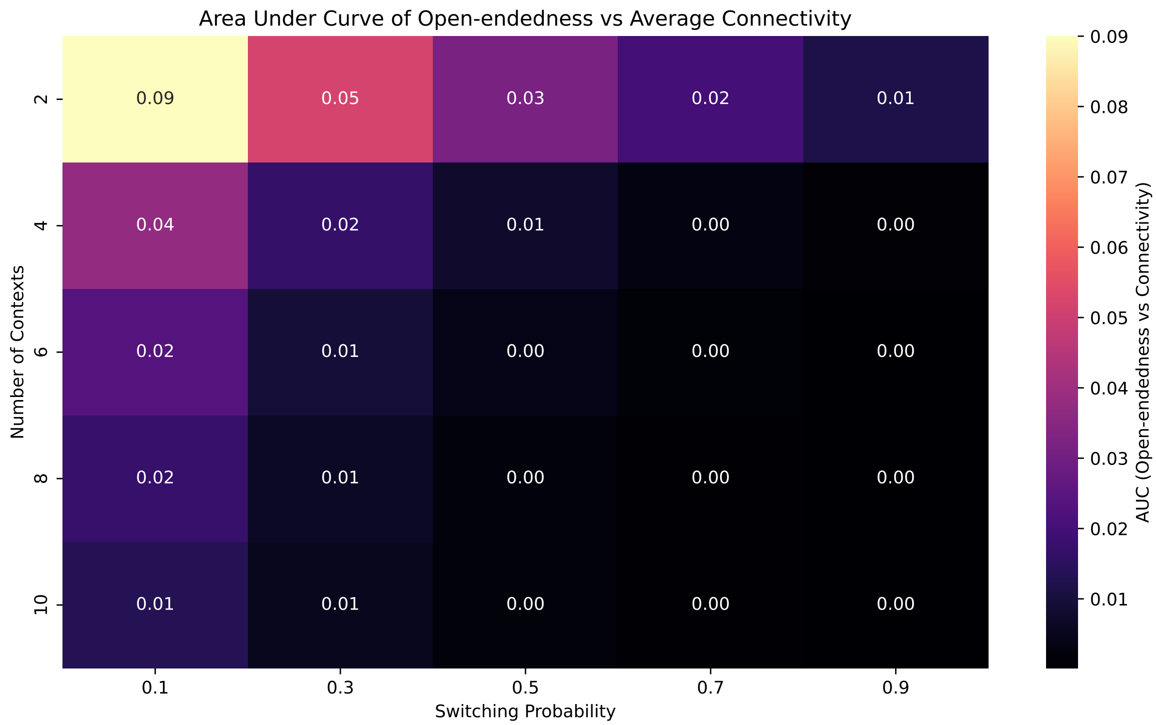

Figure 4: **AUC of $\Omega(K)$ across K for each $(\sigma, \textbf{contexts})$. The area-under-curve condenses overall performance across connectivities. The optimal setting used in the main text is annotated in the notebook (typically contexts $= 2$, $\sigma = 0.1$ for the homogeneous case).**

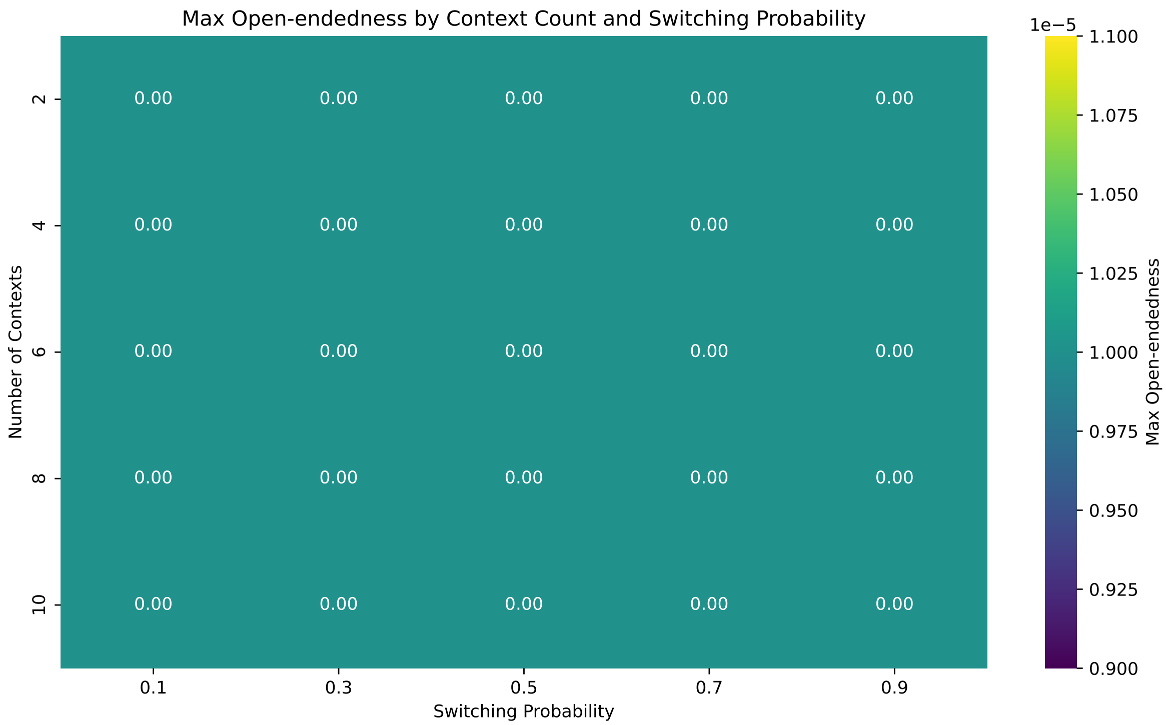

Figure 5: **PBN (σ, contexts) landscape under heterogeneity.** Max-Ω remains low throughout, consistent with asynchronous dynamics favoring point attractors; switching cannot compensate if each context quickly collapses. Color scale and axes as in Fig. 3.

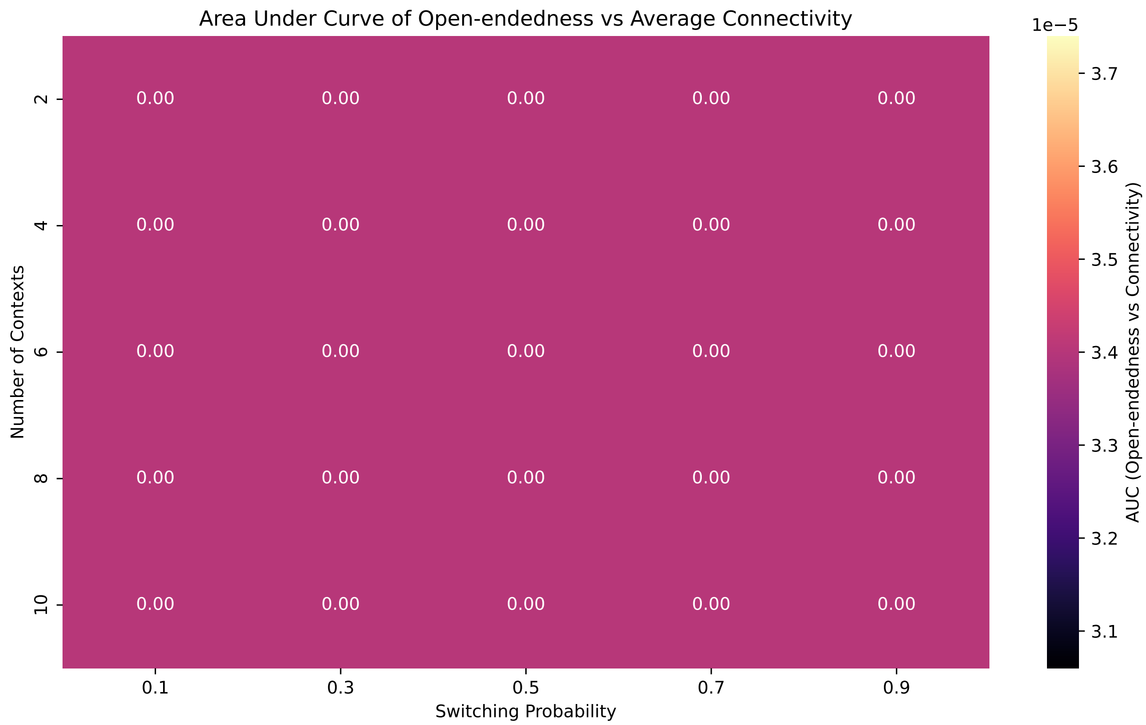

Figure 6: **PBN AUC across (σ, contexts) under heterogeneity.** Confirms the collapse of Ω across K; the setting used in the main text (`SwitchProb=0.1_Contexts=2`) is reported for completeness.

Annealed Rule Mutation (ARM): mutation probability μ

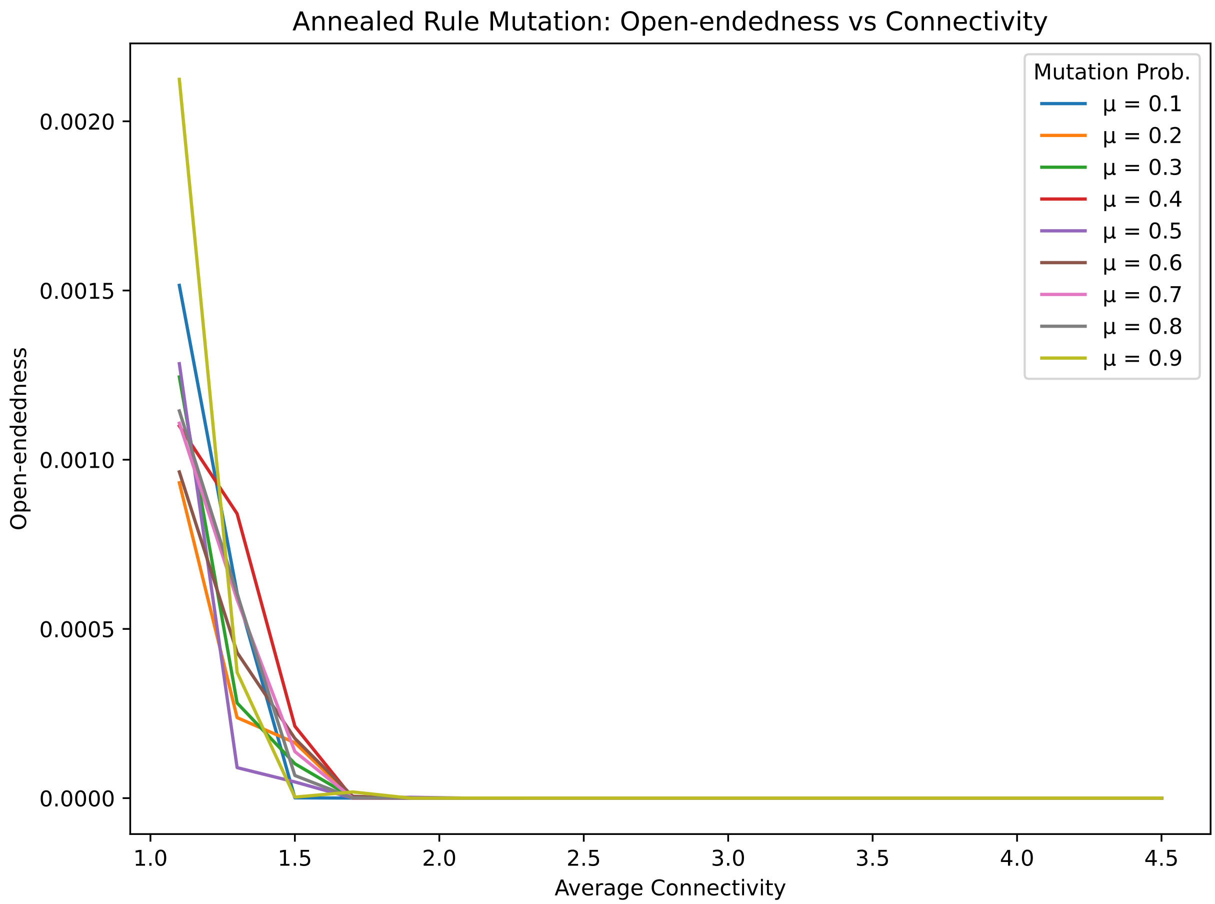

Figure 7: $\Omega(K)$ **for several mutation probabilities** μ **(legend as plotted).** Increasing μ anneals away structured attractor geometry and reduces dwell-time×cycle-length, driving Ω down. Axes: K vs. Ω.

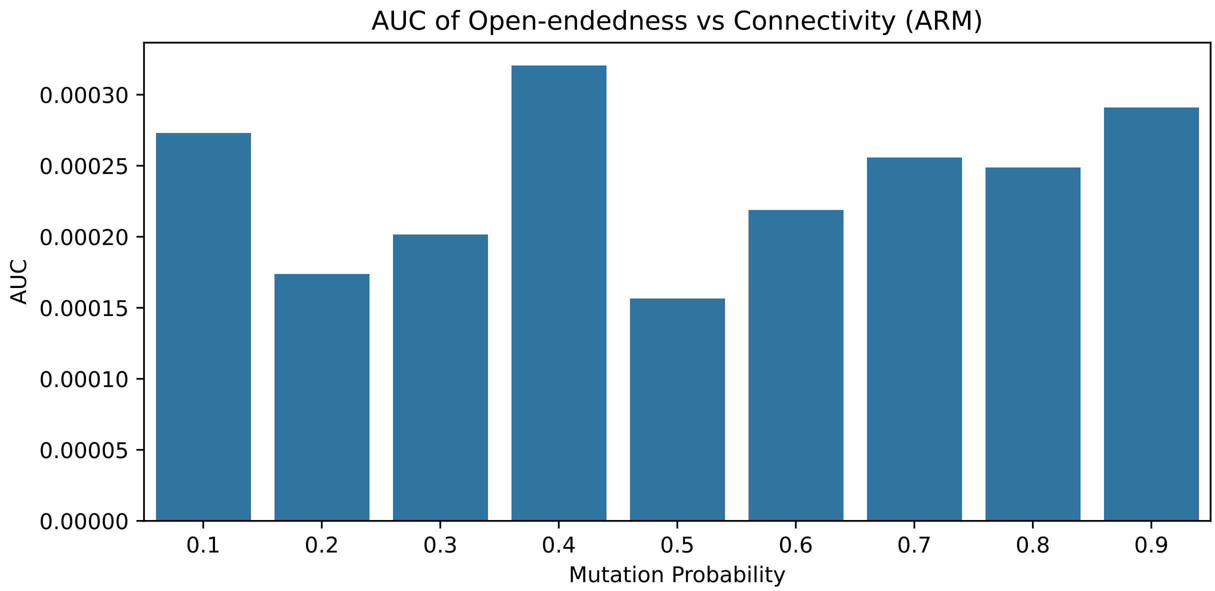

Figure 8: **AUC of $\Omega(K)$ vs. μ.** The optimal (highest AUC) μ used in the main text is indicated in the notebook (homogeneous winner: `MutationProb=0.4`). Error bars omitted; each AUC aggregates the mean over K.

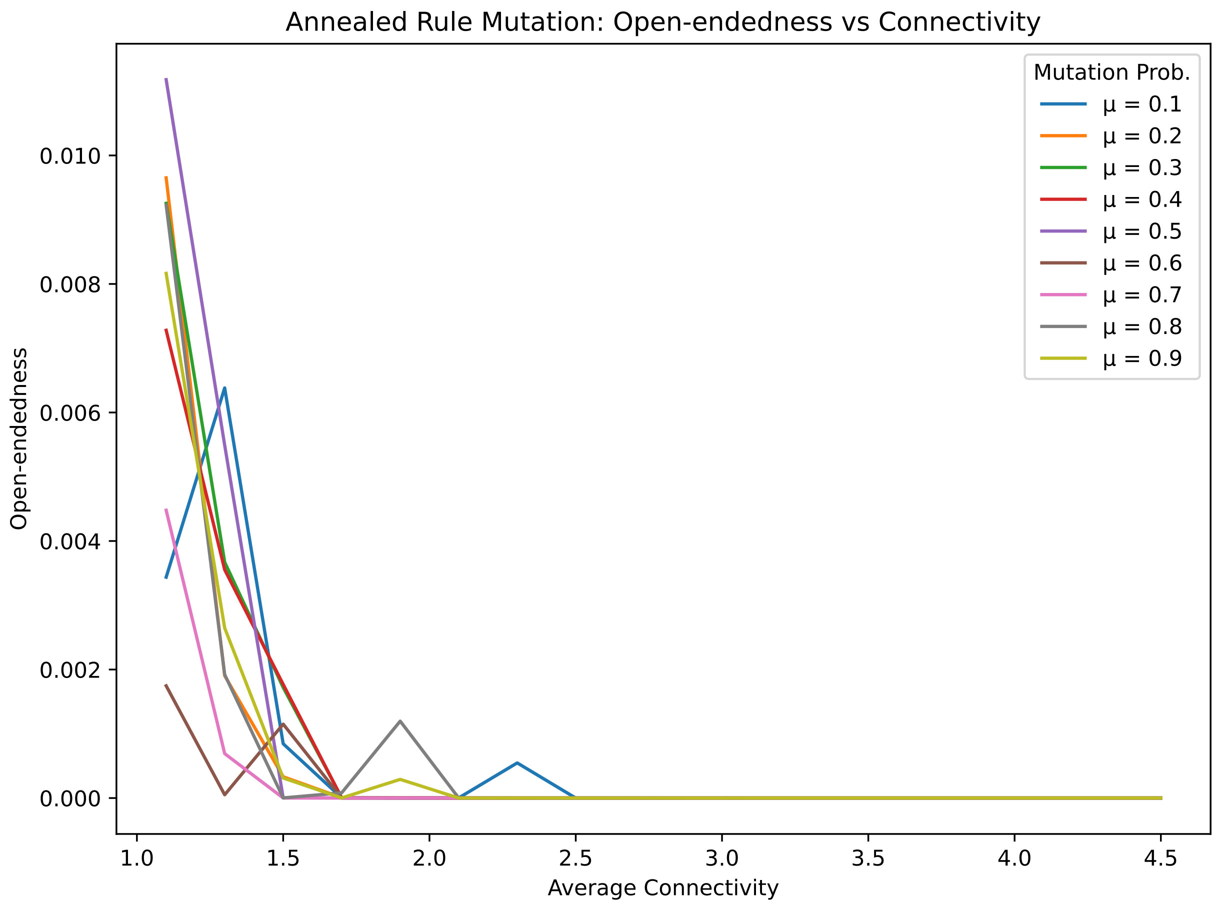

Figure 9: $\Omega(K)$ **under ARM with heterogeneity.** Asynchrony accelerates convergence to fixed points; even moderate μ suppresses Ω.

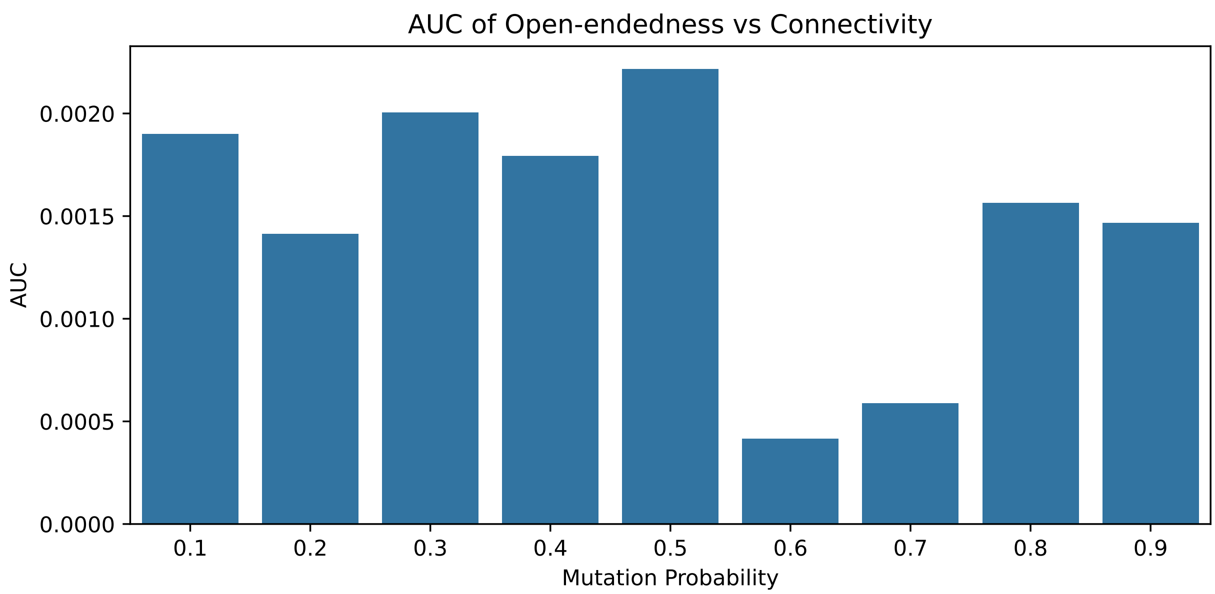

Figure 10: **AUC vs. μ under heterogeneity.** The selected setting in the main text corresponds to `MutationProb=0.5`.

Quantum-inspired logic: superposition probability s_p and entanglements e

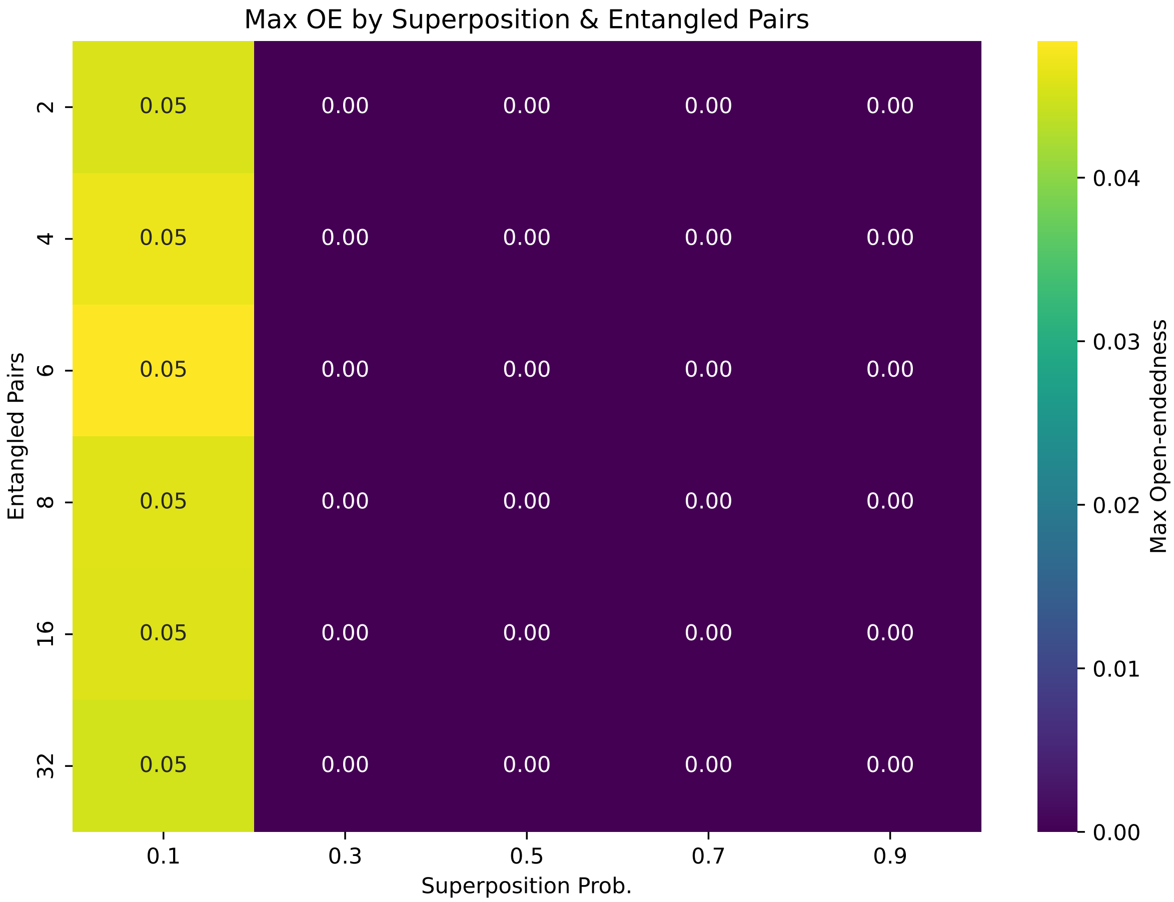

Figure 11: **Maximum Ω across K for each (s_p, e) pair.** Small s_p with a few long-range pairs yields correlated branching without washing out structure; the notebook marks the peak (`Superposition=0.1_Entangled=6`).

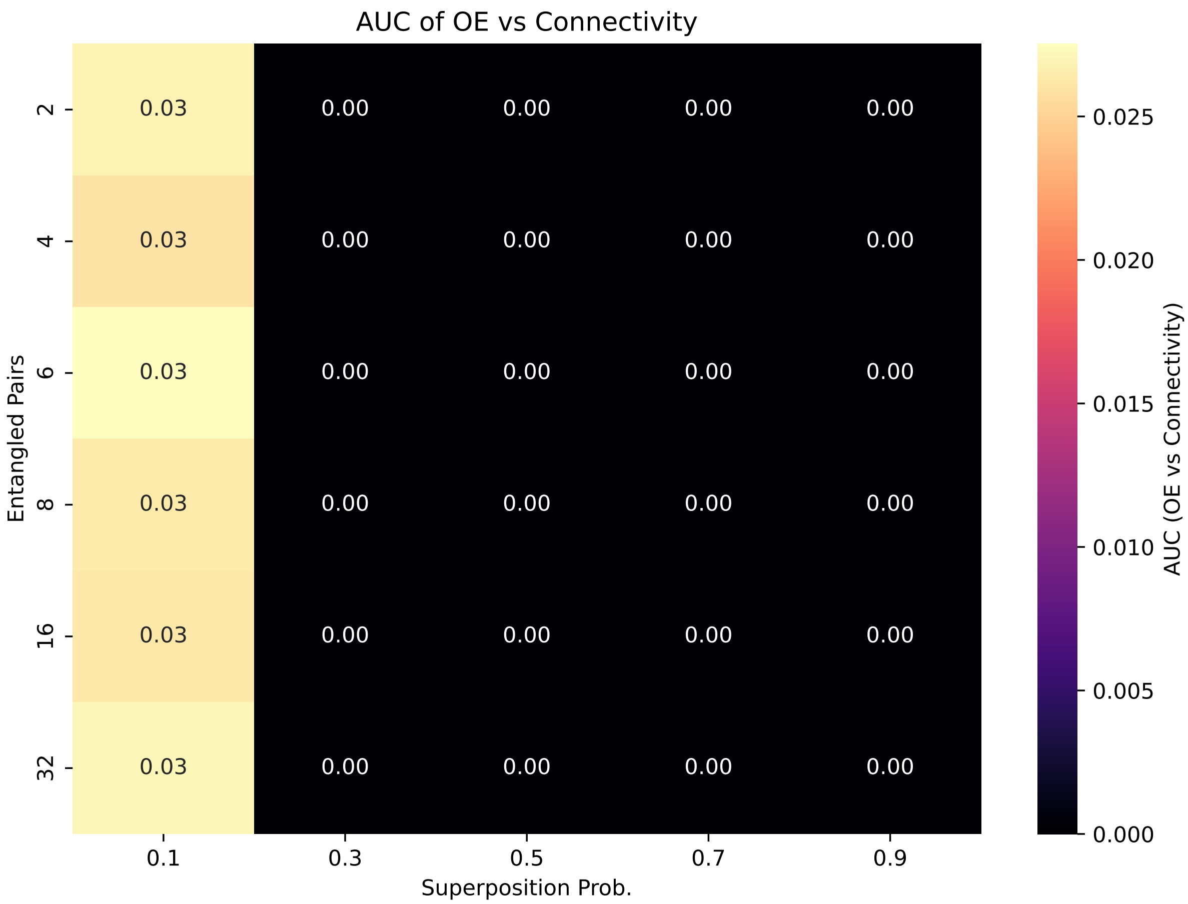

Figure 12: **AUC across** (s_p, e)**.** Summarizes overall performance across connectivities for each parameter pair; the winning combination is consistent with Fig. 11.

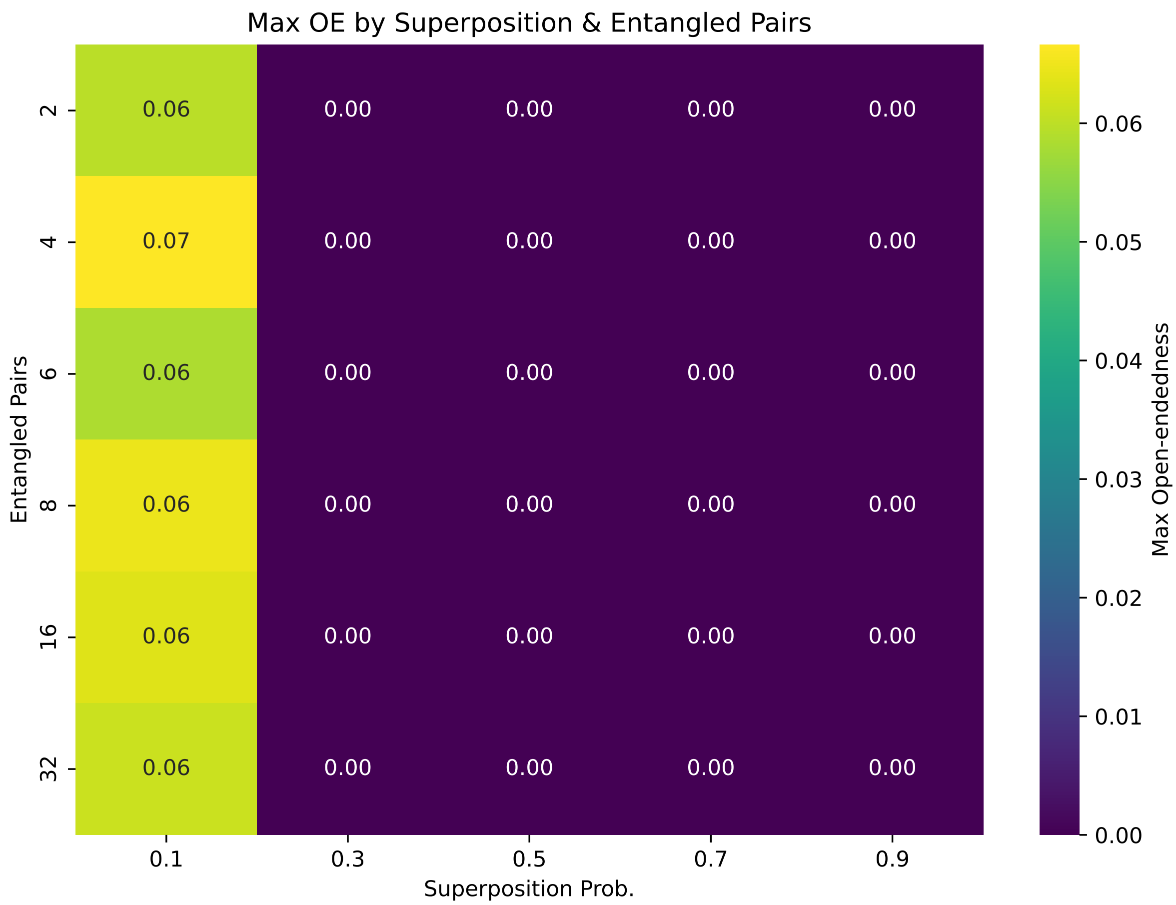

Figure 13: **Max-Ω across (s_p, e) under heterogeneity.** Sparse wiring benefits more from correlated branching; the best combination used in the main text is annotated (`Superposition=0.1_Entangled=32`).

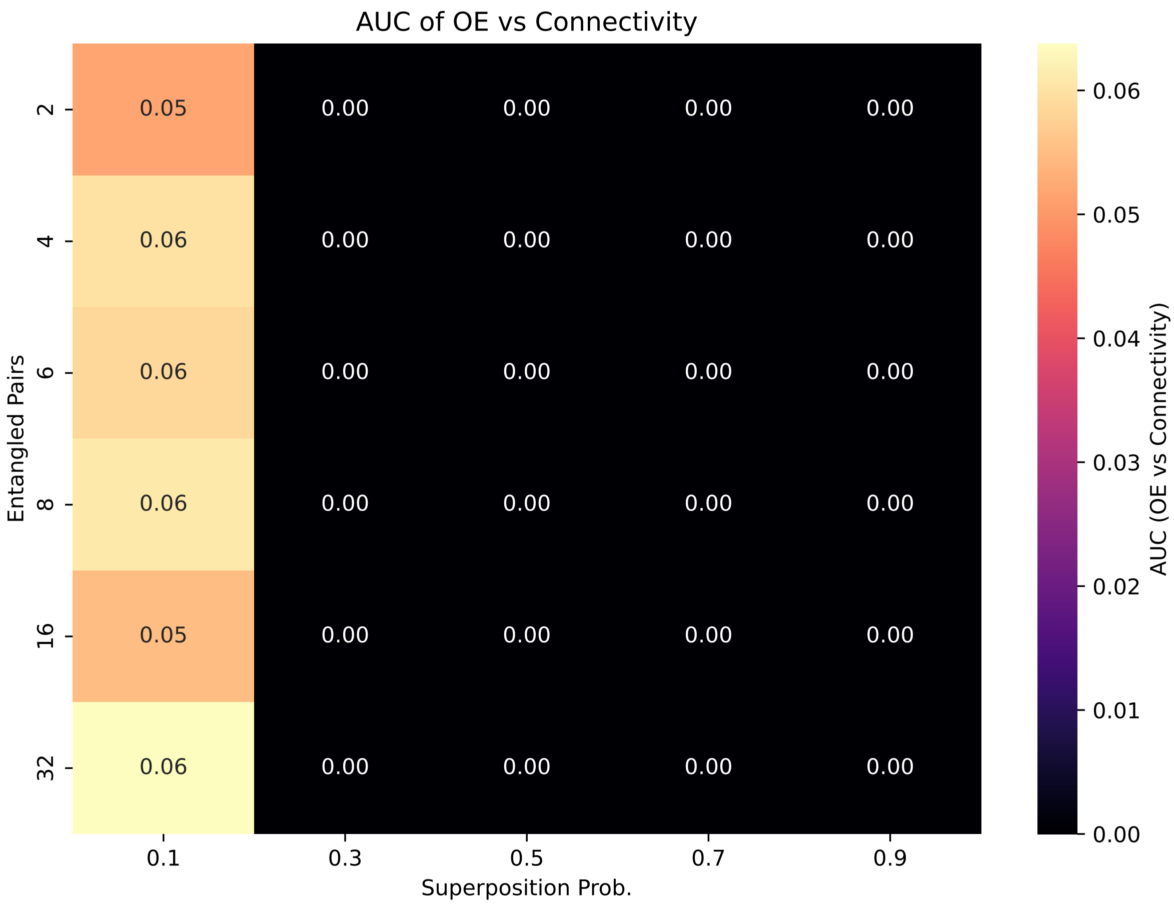

Figure 14: **AUC across** (s_p, e) **under heterogeneity.** Confirms the peak at moderate s_p and larger e.

Paraconsistent logic: contradiction probability c

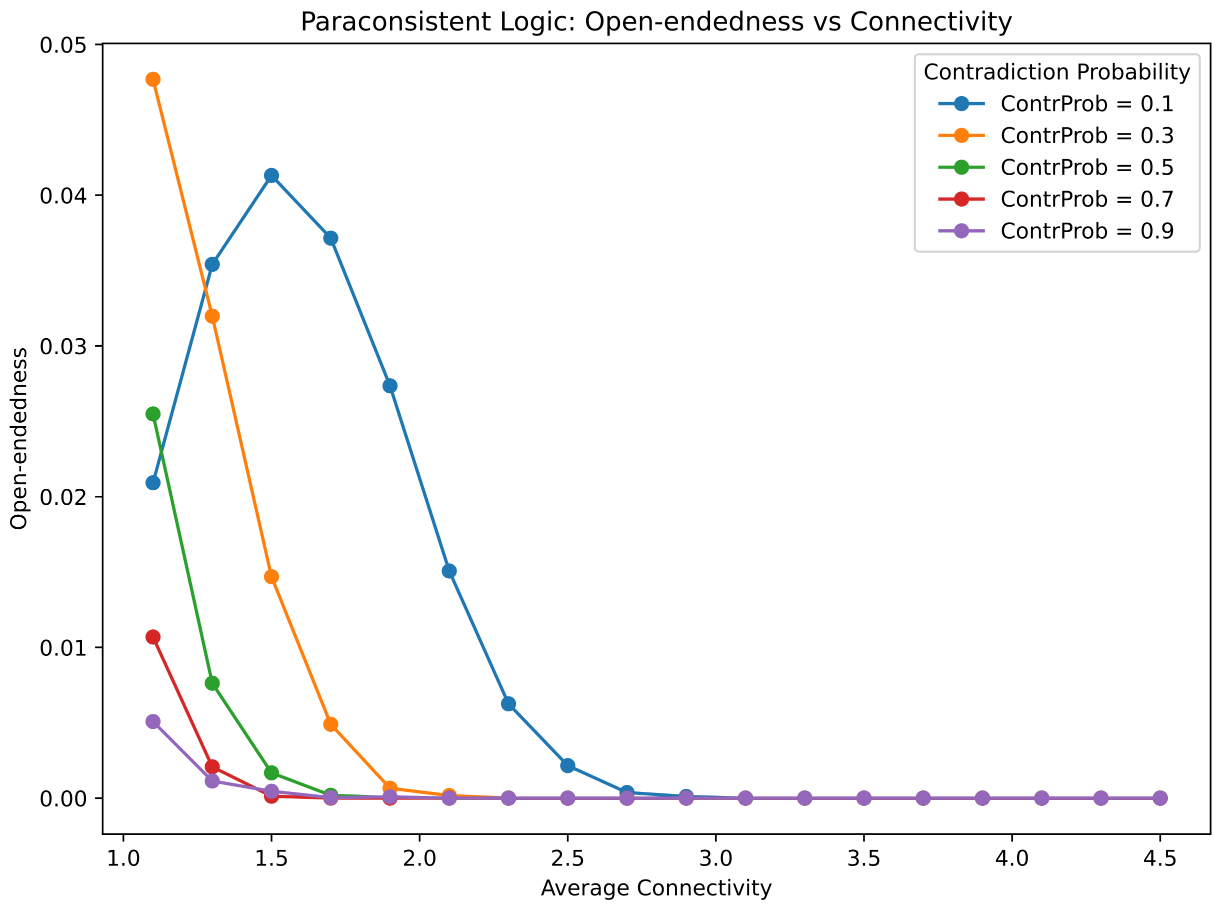

Figure 15: $\Omega(K)$ **at several contradiction probabilities** c**.** Introducing inconsistency-tolerant tokens around the order-critical region ($K \approx 2$) sustains exploratory dynamics without runaway noise.

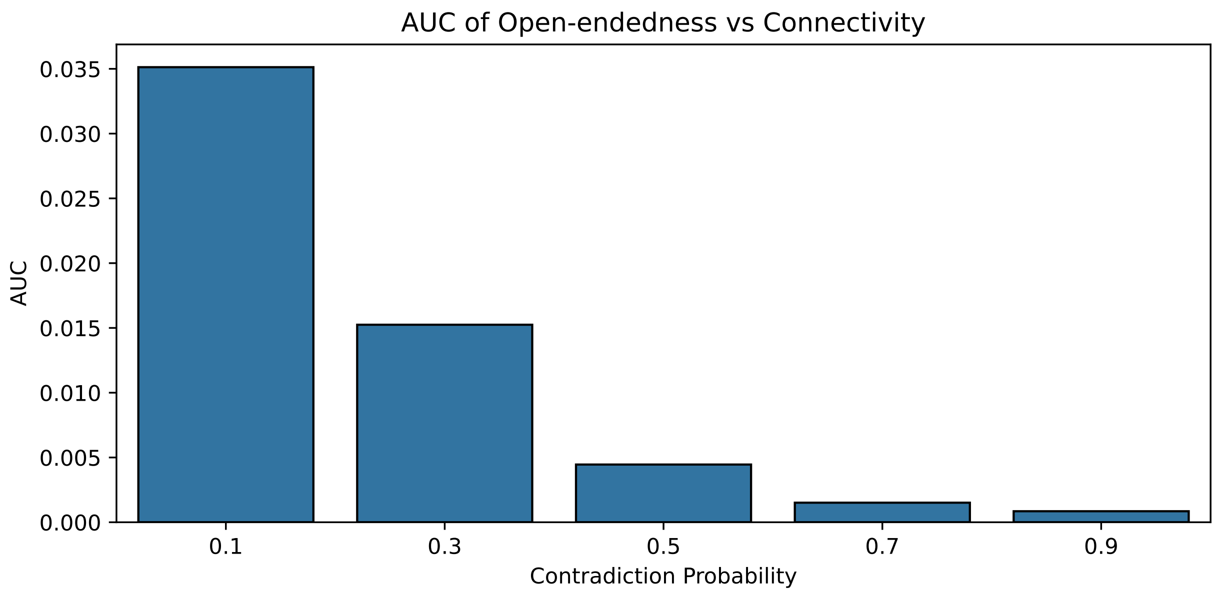

Figure 16: **AUC vs. c.** The best value used in the main text is `ContrProb=0.1`.

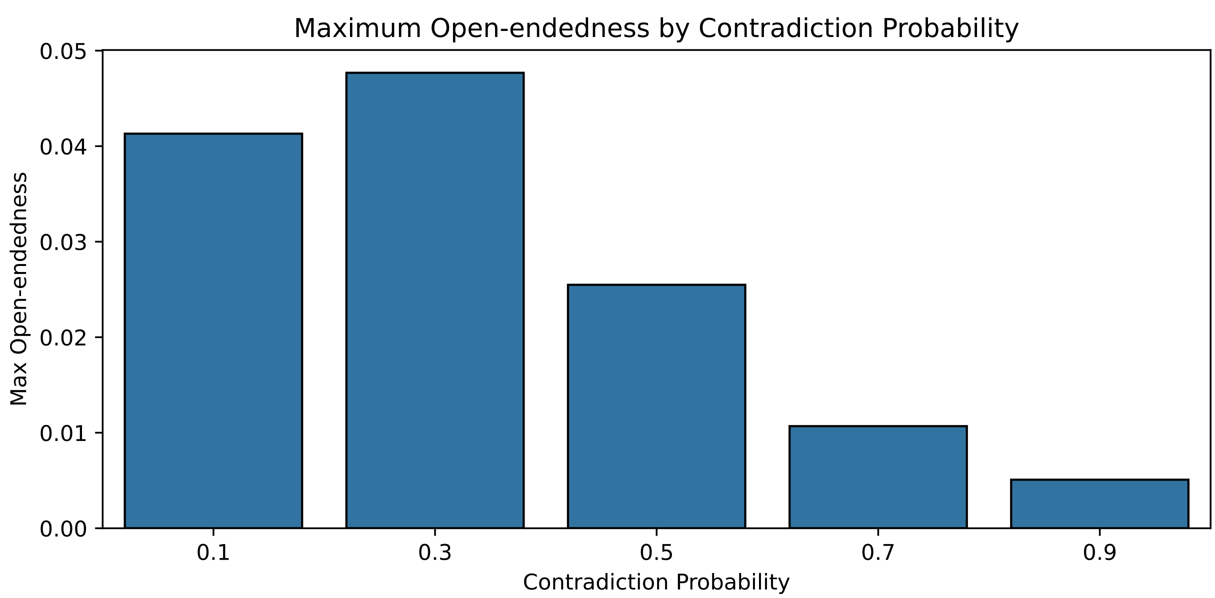

Figure 17: **Peak Ω across K at each c.** Highlights how c balances exploration (more cycles found) against stability (dwell times).

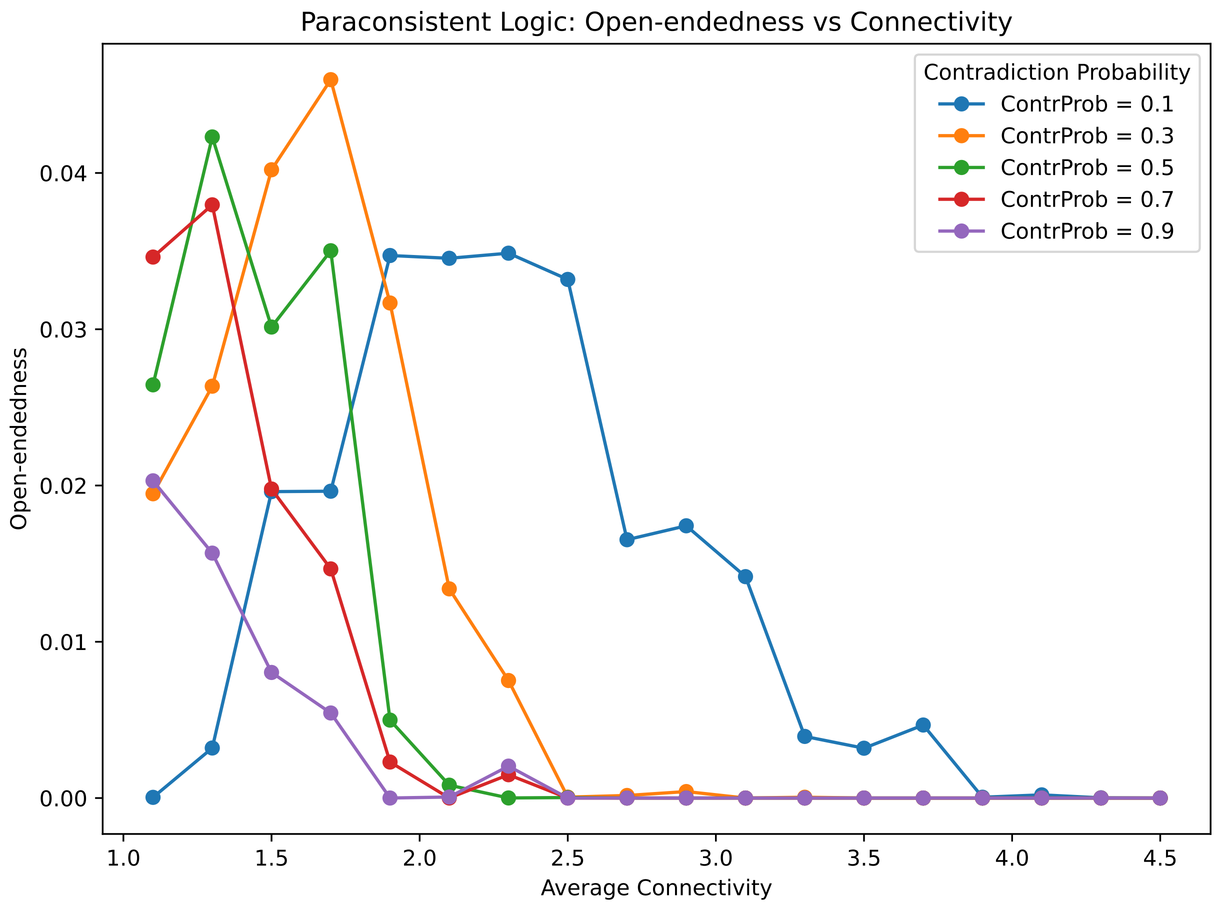

Figure 18: $\Omega(K)$ **with heterogeneity under paraconsistency.** Broad shoulder near $K \in [1.5, 2.3]$ reproduces the criticality-extending effect of heterogeneity.

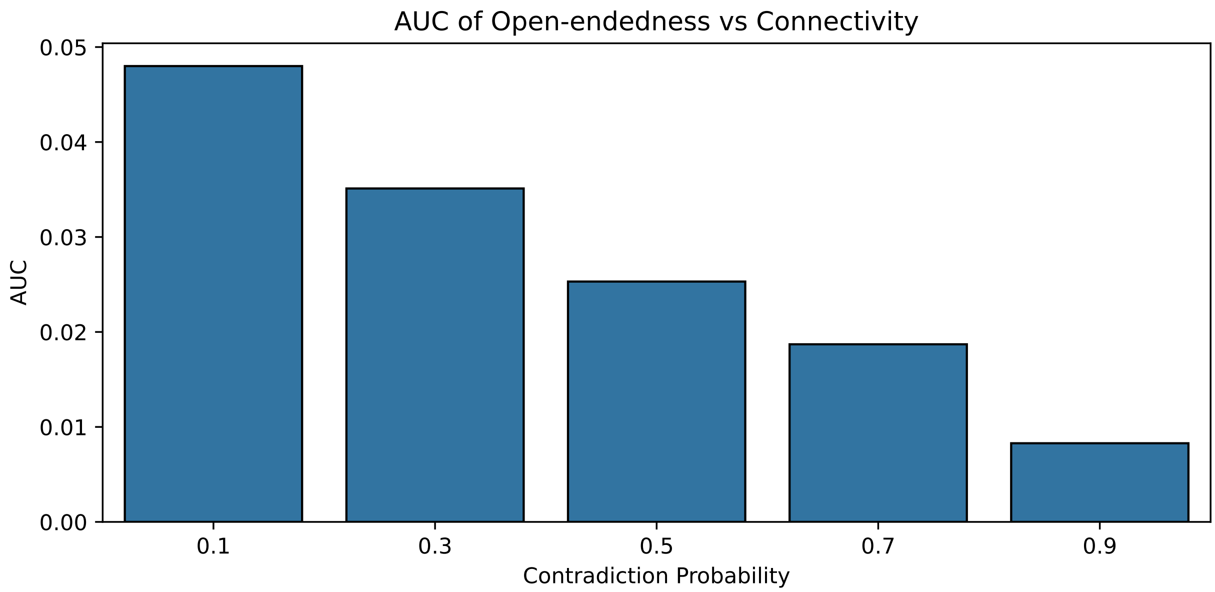

Figure 19: **AUC vs. c under heterogeneity.** Confirms the preference for small but non-zero c (best: `ContrProb=0.1`).

Modal logic: accessibility degree a, possibility p_{poss}, necessity p_{necc}

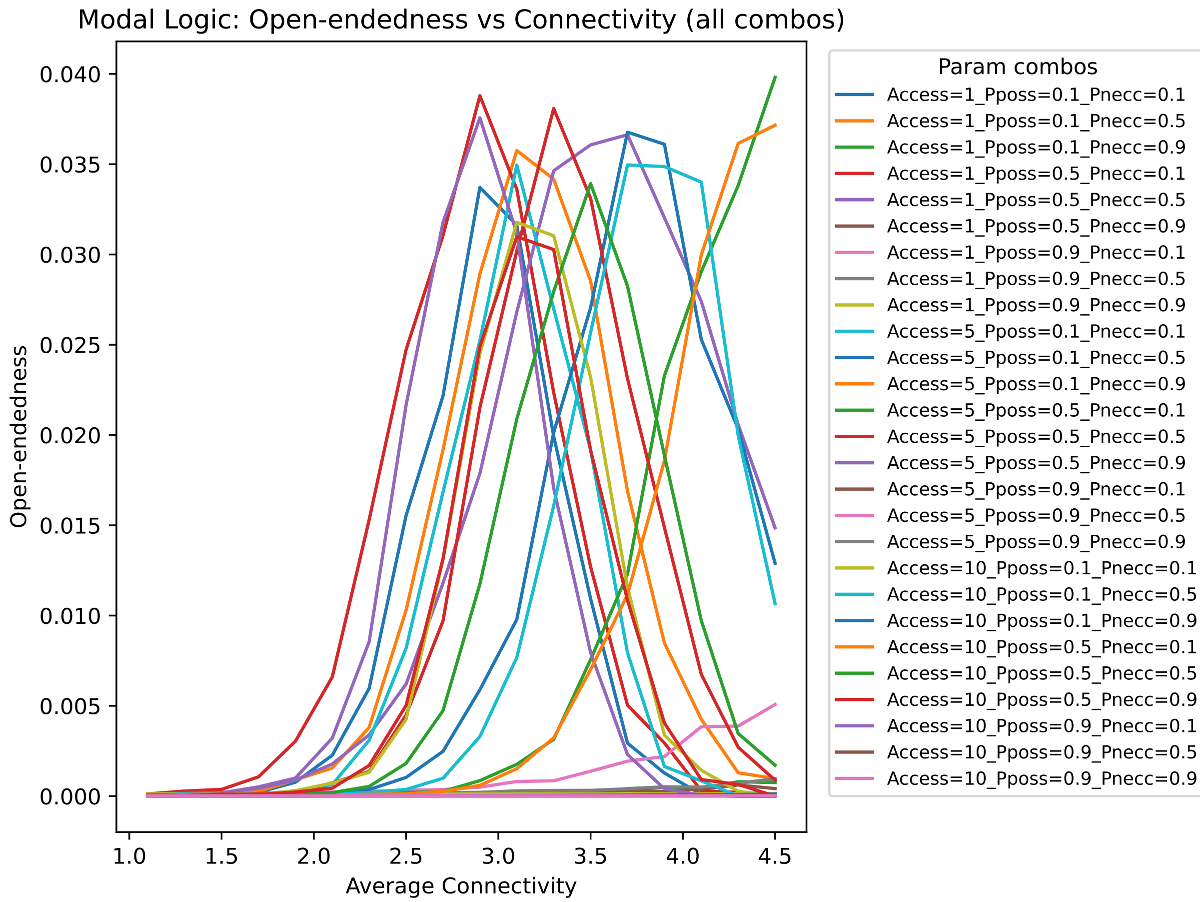

Figure 20: **All $\Omega(K)$ curves across $(a, p_{\text{poss}}, p_{\text{necc}})$ combinations.** Necessary gates act as canalizing constraints; possible gates reopen paths contextually. The best combination is `Access=1_Pposs=0.5_Pnecc=0.5`, as shown in Table 1.

Table 1: **Area under the curve, maximum OE and associated connectivity for all combinations of modal parameters (Homogeneous Case)**. Values are ranked from highest to lowest AUC.

	Access	Pposs	Pnecc	AUC	MaxOE	ConnAtMax
0	1	0.5	0.5	0.052871	0.036631	3.7
1	1	0.5	0.1	0.039701	0.038794	2.9
2	1	0.1	0.5	0.039010	0.035759	3.1
3	5	0.1	0.5	0.038415	0.036771	3.7
4	5	0.5	0.5	0.037514	0.038086	3.3
5	10	0.1	0.5	0.036748	0.034959	3.7
6	5	0.5	0.9	0.032701	0.037566	2.9
7	10	0.5	0.5	0.032658	0.033927	3.5
8	1	0.1	0.1	0.029547	0.033719	2.9
9	10	0.1	0.1	0.029440	0.031780	3.1
10	5	0.1	0.1	0.029239	0.034953	3.1
11	10	0.5	0.9	0.028516	0.030986	3.1
12	5	0.5	0.1	0.026492	0.039809	4.5
13	10	0.5	0.1	0.025501	0.037157	4.5
14	1	0.9	0.1	0.003950	0.005074	4.5
15	1	0.9	0.5	0.001013	0.000958	4.5
16	1	0.1	0.9	0.000693	0.000798	4.3
17	1	0.5	0.9	0.000636	0.000617	4.3
18	1	0.9	0.9	0.000423	0.000148	4.5
19	10	0.1	0.9	0.000137	0.000118	4.5
20	5	0.1	0.9	0.000081	0.000040	4.3
21	10	0.9	0.9	0.000057	0.000021	4.3
22	10	0.9	0.5	0.000048	0.000017	4.3
23	10	0.9	0.1	0.000043	0.000015	4.1
24	5	0.9	0.5	0.000042	0.000015	4.5
25	5	0.9	0.9	0.000042	0.000013	3.7
26	5	0.9	0.1	0.000042	0.000014	4.3

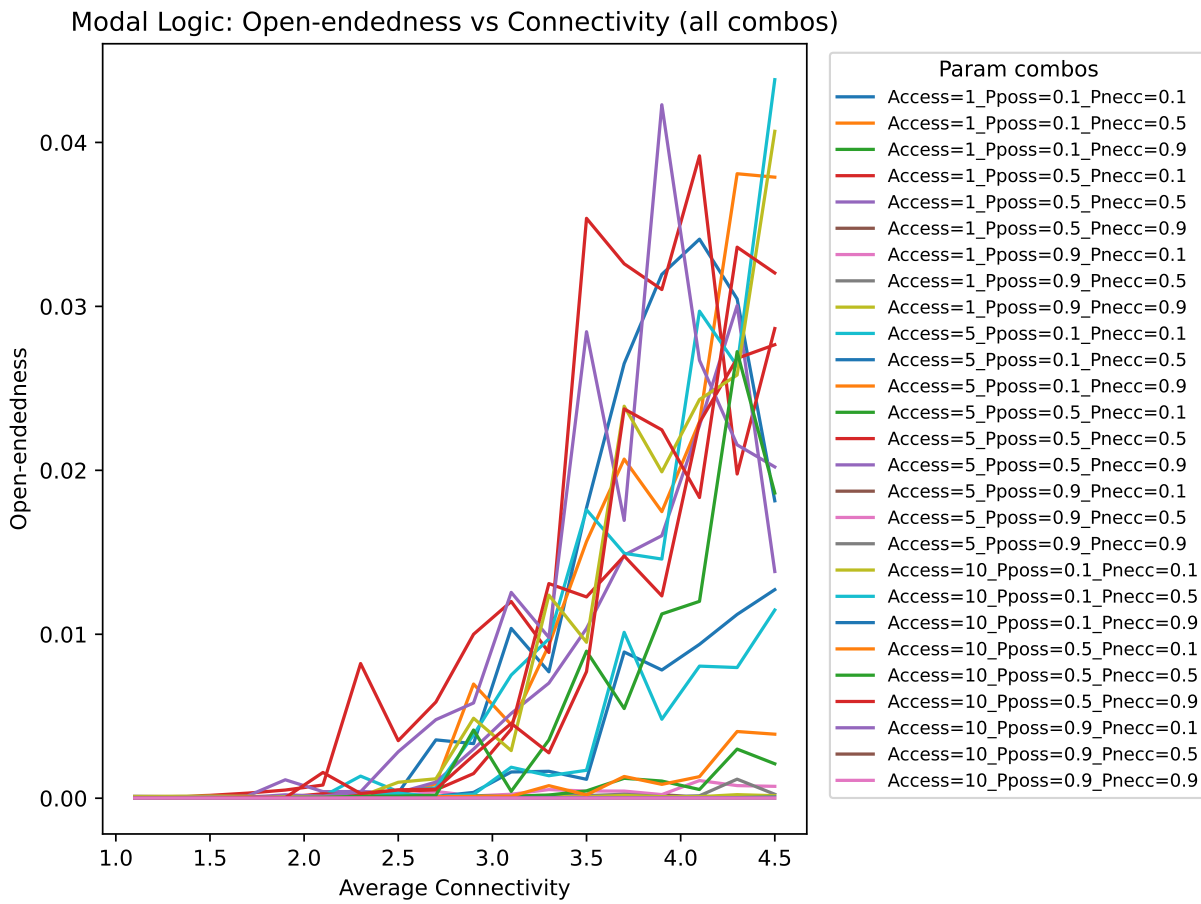

Figure 21: $\Omega(K)$ **across** $(a, p_{\text{poss}}, p_{\text{necc}})$ **under heterogeneity.** The winning combo used in the main text is `Access=1_Pposs=0.5_Pnecc=0.1`, which preserves metastable corridors at high K.

Table 2: **Area under the curve, maximum OE and associated connectivity for all combinations of modal parameters (Heterogeneous Case)**. Values are ranked from highest to lowest AUC.

	Access	Pposs	Pnecc	AUC	MaxOE	ConnAtMax
0	1	0.5	0.5	0.052871	0.036631	3.7
1	1	0.5	0.1	0.039701	0.038794	2.9
2	1	0.1	0.5	0.039010	0.035759	3.1
3	5	0.1	0.5	0.038415	0.036771	3.7
4	5	0.5	0.5	0.037514	0.038086	3.3
5	10	0.1	0.5	0.036748	0.034959	3.7
6	5	0.5	0.9	0.032701	0.037566	2.9
7	10	0.5	0.5	0.032658	0.033927	3.5
8	1	0.1	0.1	0.029547	0.033719	2.9
9	10	0.1	0.1	0.029440	0.031780	3.1
10	5	0.1	0.1	0.029239	0.034953	3.1
11	10	0.5	0.9	0.028516	0.030986	3.1
12	5	0.5	0.1	0.026492	0.039809	4.5
13	10	0.5	0.1	0.025501	0.037157	4.5
14	1	0.9	0.1	0.003950	0.005074	4.5
15	1	0.9	0.5	0.001013	0.000958	4.5
16	1	0.1	0.9	0.000693	0.000798	4.3
17	1	0.5	0.9	0.000636	0.000617	4.3
18	1	0.9	0.9	0.000423	0.000148	4.5
19	10	0.1	0.9	0.000137	0.000118	4.5
20	5	0.1	0.9	0.000081	0.000040	4.3
21	10	0.9	0.9	0.000057	0.000021	4.3
22	10	0.9	0.5	0.000048	0.000017	4.3
23	10	0.9	0.1	0.000043	0.000015	4.1
24	5	0.9	0.5	0.000042	0.000015	4.5
25	5	0.9	0.9	0.000042	0.000013	3.7
26	5	0.9	0.1	0.000042	0.000014	4.3

Notes on computation and data flow

- **Metric extraction.** The notebooks rely on the extractor that computes (V, P, KD) and $\Omega = KD/T^2$ from streams of states, ensuring correctness for both CPU and GPU paths.
- **GPU/CPU paths.** Long runs stream trajectories on the GPU when available; modest horizons use CPU multiprocessing. The cycle–tail shortcut is used for very large T when appropriate to avoid unnecessary simulation.
- **AUC definition.** Unless otherwise indicated, AUC is computed by trapezoidal integration of the mean $\Omega(K)$ curve over the K grid.

Abbreviations

ARM: Annealed Rule Mutation; PBN: Probabilistic Boolean Network; K: average in-degree; T: number of time steps; AUC: area under the $\Omega(K)$ curve.